35th Annual International Conference of the IEEE EMBS
Osaka, Japan, 3 - 7 July, 2013

Droplet Backside Exposure for Making Slanted SU-8 Microneedles

Ki Yong Kwon, *Student member*, *IEEE,* Xiaopeng Bi, and Wen Li, *Member, IEEE*

***Abstract*—This paper presented a droplet backside exposure (DBE) method for making slanted microneedle structures on a flexible polymer substrate. To demonstrate the feasibility of the DBE approach, SU-8 microneedle arrays were fabricated on polydimethylsiloxane (PDMS) substrates. The length of the microneedles was controlled by tuning the volume of the SU-8 droplet, utilizing the wetting barrier phenomenon at a liquid-vapor-hydrophilic surface-hydrophobic surface interface . The experimental results showed excellent repeatability and controllability of the DBE method for microneedle fabrication. Analytical models were also studied to predict the dimensions of the microneedles, which agreed with the experimental data.**

I. Introduction

Microneedles have been widely used as an interface between a biomedical system and biological tissue/organism, for a variety of applications such as transdermal drug delivery [1] and biosensors [2]. Many microfabrication techniques have been developed for making both in-plane and out-of-plane microneedles, using various materials such as metal, polymer, and glass [1]. Specifically, out-of-plane microneedles made of polymers or glass show excellent optical properties and can potentially serve as waveguides for light transmission [3]. In electrophysiology and clinical neuroscience, particular interest is to utilize such microneedle waveguides to direct light for optical stimulation of neurons, based on an emerging optogenetics technology [4]. We recently reported a multi-LED array with integrated individually addressable μ-LED chips and microneedles, which effectively minimized the scattering of LED lights in the brain tissue and leaded to high spatial resolution and precise light delivery to the target neurons [5].

However, these microneedles have a single-length shank, which greatly limits the depth selectivity of the optical stimulation. In fact, for the application of central nervous system (CNS) stimulation, delivering optical stimulation at various cortical layers is critical. Moreover, peripheral neuroprosthetic interface requires accessing multiple independent motor neuron subpopulations in peripheral nerves or muscles to restore motor and sensory functions. Recently, a micro-machined three-dimensional (3-D) optrode array, called Utah Slant Optrode Array (USOA) neural interface, was developed to provide comprehensive access for infrared neural stimulation [3]. However, the complex fabrication process of the USOA involved dicing and etching a thick glass substrate and required a specialized machine and materials. The rigidity of the USOA also limited accessing peripheral nerves with small curvatures.

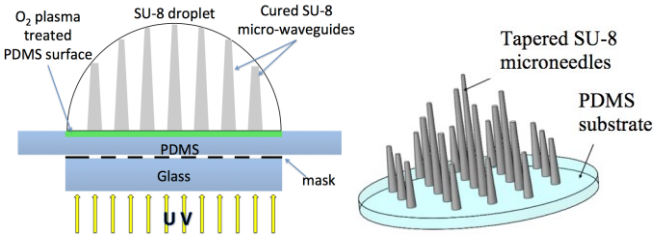

Figure 1. Principle of the proposed SU-8 droplet backside exposure (DBE) method and a 3-D slanted waveguide array

To address these challenges, we proposed a flexible, slanted waveguide array with varying-length microneedles. Within many available fabrication methods, polymer (SU-8) based fabrication technique utilizing a backside exposure lithography was considered, because of the high refractive index of SU-8, the simplicity of the fabrication technique, and the biocompatibility suitable for bio-MEMS applications [6]. While the adapted method allows length control with different size of mask, independent control of dimensions (e.g. base and tip sizes, height) of the microneedle is not possible [2]. Control of these parameters is critical in waveguide design, since these parameters determine the coupling efficiency, irradiance and total flux of the needle-shaped waveguide [7].

In this work, a new fabrication method, called droplet backside exposure (DBE), is developed, utilizing the height variance in the profile of a droplet structure to create slanted microneedles (Fig. 1). This technique can independently control the length, and tip/bottom diameters of individual microneedles without using a specialized machine or complex fabrication techniques. In the following sections, we will detail the principle of the proposed method, fabrication steps of the slanted waveguide array, and experimental results to prove the practicality of the fabrication method.

II. Methods

Our proposed DBE technique takes advantage of a wetting barrier phenomenon occurred at a four-phase interface [8]. Generally, the shape of a liquid droplet on a homogenous solid substrate is primarily governed by the surface free energy of the substrate. However, for a four-phase interface such as a vapor-liquid-hydrophilic surface-hydrophobic surface interface, the spreading of the liquid is restricted by the wetting barrier formed at the boundary between the hydrophilic region and the hydrophobic region. Consequently, the contact angle of the droplet can vary within a certain

*Research supported by National Science Foundation and Michigan State University.

K. Kwon, X. Bi, and W. Li are with the Electrical and Computer Engineering Department, Michigan State University, East Lansing, MI 48824 USA (phone: +1-517-353-7832, e-mail: kwonki3@egr.msu.edu, wenli@egr.msu.edu).

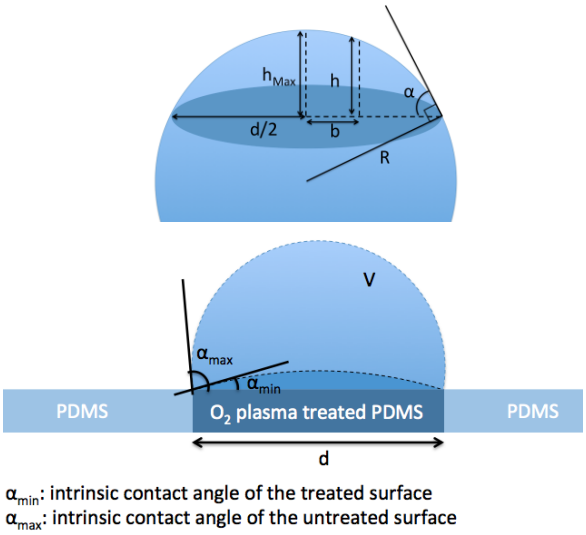

Figure 2. Geometry of ideal partial sphere droplet

range, with a maximum contact angle corresponding to the equilibrium contact angle of the hydrophobic surface.

Based on this principle, we designed an analytical model to determine the maximum volume of SU-8 sustained in a pre-defined pattern as well as to predict the length variation of microneedles. As show in Fig. 2, our model assumed the droplet had a perfect spherical shape with a diameter of R. At equilibrium, the volume of the SU-8 solution can be calculated using the following equation:

$$V = \frac{1}{3}\pi R^3(2 - 3\sin(90-\alpha) + sin^3(90-\alpha)) \quad (1)$$

where V is the actual volume of SU-8 delivered to the substrate and α is the equilibrium contact angle of the SU-8 droplet after pre baking. The diameter of the interface between the droplet and the O_2 plasma treated polydimethylsiloxane (PDMS) surface, d, is pre-defined and the relationship between R and d is given below:

$$R = \frac{d}{2\cos(90-\alpha)} \quad (2)$$

By substituting R with d in Eqn. 1, the liquid volume can be rewritten as a function of the pre-defined interfacial diameter and the equilibrium contact angle of droplet.

$$V = \frac{1}{12}\pi d^3 \frac{(2+\cos\alpha)(1-\cos\alpha)^2}{\sin^3\alpha} \quad (3)$$

Once a shape of the droplet is determined by SU-8 volume, three parameters, tip diameter, bottom diameter, and the length of the microneedle, can be controlled by the mask diameter and the distance from the center of the droplet of the mask aperture. The base diameter of the microneedle is associated with the diameter of the mask [2], and the tip size is closely linked with the tapered angle of the microneedle and the thickness of the SU-8 layer on top of the mask aperture. Since the tapered angle is controlled by the distance between the absorber on the photo mask and the top of the SU-8 [6], the only controllable parameter is the thickness of the SU-8 layer. Because the thickness of the SU-8 varies in a predictable manner in the SU-8 droplet structure, the length

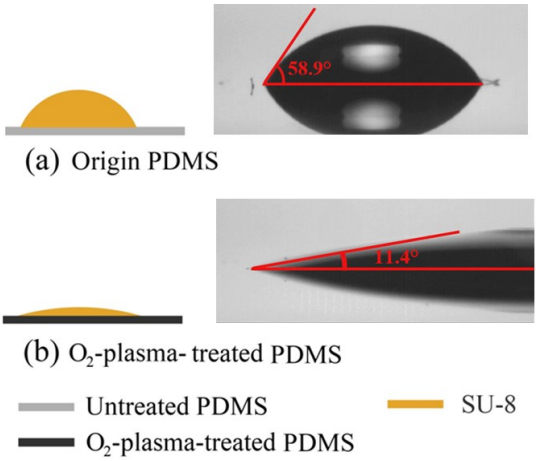

Figure 3. The wetting behavior of the SU-8 on (a) a untreated PDMS substrate and (b) a O_2-plasma-treated PDMS. The contact angles were measured by a contact angle analyzer.

and the tip diameter can be designed by tuning the distance between the mask opening and the center of the droplet.

h_{Max} is the maximum height of the droplet and it can be estimated using a trigonometric relationship of R and α shown in Fig. 2.

$$h_{Max} = R - \frac{d}{2}\tan(90-\alpha) = R - \frac{d}{2\tan\alpha} \quad (4)$$

Once the h_{Max} is estimated from the applied volume, a parameter h, which is a height at the distance b from the center of the droplet, can be calculated using (details are found in [9])

$$h = \frac{\sqrt{\left(\frac{d}{2}\right)^4 + h_{Max}{}^2\left(2\left(\frac{d}{2}\right)^2 - 4b^2 + 1\right) - \left(\frac{d}{2}\right)^2 + h_{Max}^2}}{2h_{Max}} \quad (5)$$

III. Fabrication

PDMS was selected as the flexible substrate as it can be effectively modified to super hydrophilic through oxygen (O_2) plasma treatment. Prior to microneedle fabrication, the equilibrium contact angles of the SU-8 on both intact and plasma-treated PDMS substrates were measured to guide the design of the microneedle lengths. As shown in Fig. 3(a) and 3(b), the contact angles on hydrophobic and hydrophilic PDMS substrates were ~58.7° and ~10°, respectively. With an interfacial diameter of 7 mm, h_{max} was estimated to range from 306 µm to 1968 µm. Fig. 4 depicts the fabrication process flow of the DBE method. Specifically, (1) a well-mixed PDMS (Polydimethylsiloxane, Sylgard 184) pre-polymer components in a 10:1 ratio was degased under vacuum until no bubbles appear (20~ 30 minutes). On a clean 3" glass wafer, ~80 µm thick PDMS was spin coated (800 rpm for 40 sec). After the PDMS was cured for 40 min at 95 °C, photoresist (PR, S1813) was spun on the PDMS (2000 rpm for 40 sec). Droplet base patterns with various diameters (3~7 mm) were patterned on PR layer by photolithography. The exposed PDMS surface was then treated with O_2 plasma to modify the surface wettability. (2) After removing the PR masking layer, SU-8 (SU-8 3005) was dispensed on the top of the plasma treated PDMS surface using a micropipette (3) and then

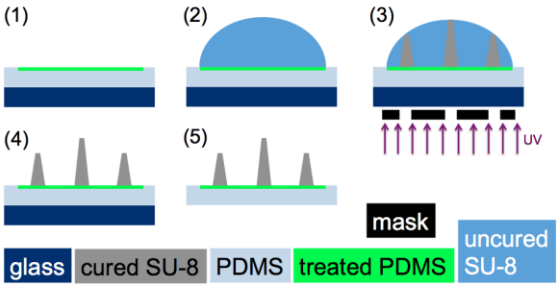

Figure 4. Fabrication process

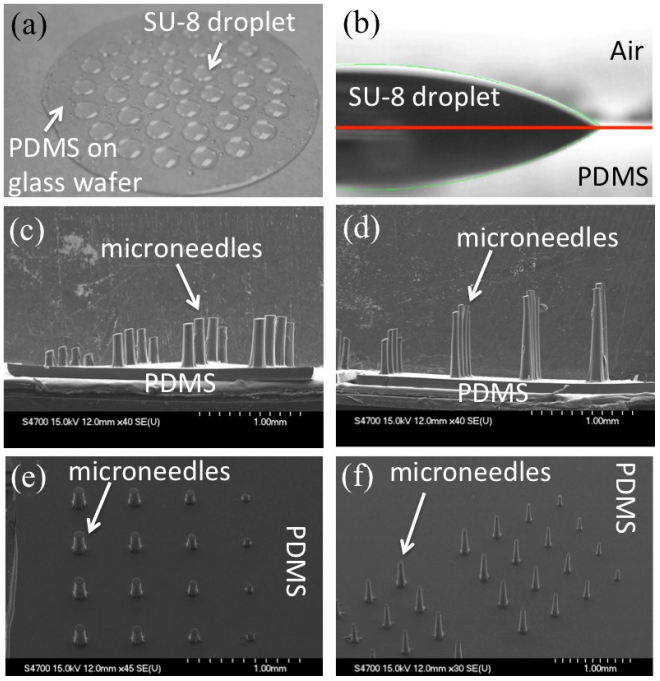

Figure 5. Captured images in the proposed DBE process: (a) dispensed SU-8 droplets on PDMS. (b) the surface profile of the SU-8 droplet. SEM images of (c) the profile view and (e) aerial view of the microneedles with 24.8° contact angle. SEM images of (d) the profile view and (f) aerial view of the microneedles with 35.2° contact angle.

patterned with the backside exposure to form the slanted microneedle structure. (4) After SU-8 development, the slanted microneedles were polished with O_2 plasma etching. (5) Finally the flexible microneedle array was released from the glass wafer.

IV. RESULTS AND DISCUSSIONS

SU-8 droplets with 7 mm diameter were dispensed on 3' glass wafer in Fig.5 (a) and the contact angle of the droplet was measured using a contact angle analyzer as shown in Fig. 5 (b). Two sets of waveguide arrays with 15 µL and 22 µL were fabricated with the proposed DBE and the SEM images of the profiles in different angles were shown in Fig.5 (c) (and (e) with 24.8° angle) and (d) (and (f) with 35.2° angle) respectively. In this session, viability and consistency of the proposed method were investigated with finite element simulation and an empirical approach.

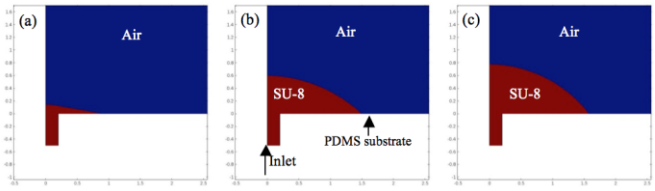

Figure 6. Dynamic contact angles simulated at t = 0.02 s (a), t = 0.16 s (b), and t = 0.25 s (c) are 11.77°, 45.00°, and 56.31°, respectively.

A. Maximum droplet volume

Finite element simulation was performed with COMSOL Multiphysics 4.3 using the Laminar Two-Phase Flow (Level Set) model in order to verify the maximum droplet volume derived from the abovementioned analytical model. In this case, the diameter of the droplet was 3 mm and the surface contact angles of the SU-8 droplet was about ~10° on the plasma treated PDMS and ~58.7° on the untreated PDMS, measured by a contact angle analyzer. The simulation used 7.95 mm^2/s for the kinematic viscosity of SU-8 3005 at an elevated temperature (between 60 °C and 95 °C) [10]. We assumed the SU-8 density of 1.075 g/cm3 and the surface tension of about 48 mN/m [10], [11]. The mass flow rate of the inlet was 2.15×10-5 kg/s. Dynamic contact angle was recorded for 0.5 s at an interval of 0.005 s, and the simulation results at 0.02, 0.16 and 0.25 s were shown in Fig. 6.

A transition of the dynamic contact angle was observed at t = 0.16 s, corresponding to a maximum volume of ~ 3.2 µL. This value agreed with our prediction based on Eqn. 3, which gave the maximum volume of the droplet at αmax of 3.23 µL. The maximum contact angle of the SU-8 droplet was 56.31° on the hydrophobic PDMS surface, similar to the value obtained from the contact angle analyzer. It was noticed that evaporation of solvent/liquid affected the dynamic contact angle during the transient simulation, which will need to be further investigated.

B. Control of microneedle length

SU-8 droplet with a diameter of 7 mm was used to study the relationship between the droplet volume and the microneedle height. In this case, SU-8 droplets were dispensed on the O_2 plasma treated PDMS surface. The droplet volume ranged from 10 to 27 µL with a 0.5 µL increment. During the DBE, the mask aperture size for the microneedle was varied from 140, 120, 100, to 80 µm (in diameter), corresponding to a distance from the droplet center of 780, 1440, 2130, and 2830 µm, respectively. 10 microneedle arrays were made for each volume size and their lengths, measured from the SEM images, were compared with the estimated values from Eqn. 5. As shown in Fig. 7 (a)-(d), the measured heights of the microneedles were consistently lower than the estimated values, which was primarily due the shrinkage of the SU-8 after post-baking. Considering a polymer shrinkage after post-baking reported in [12], a new estimation was made which well fitted the measured values.

Consistency of the DBE with fixed droplet volume was also investigated. 10 waveguide arrays were made with same mask specification described above.

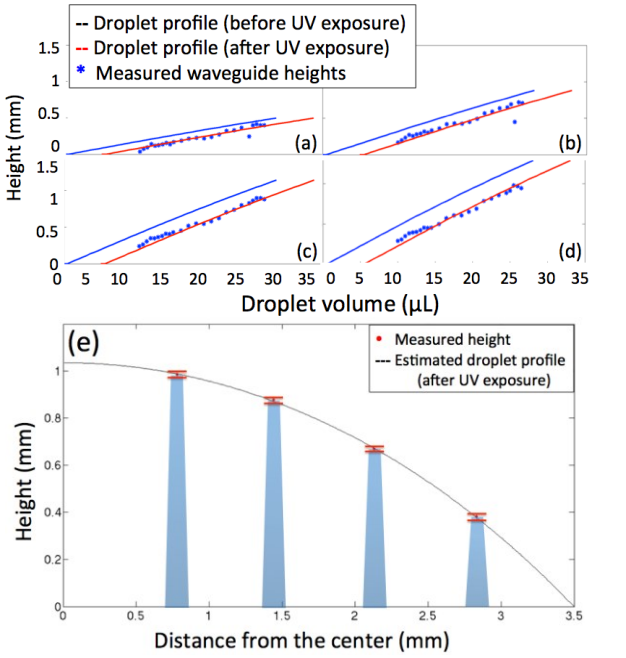

Figure 7. Estimated microneedle heights before (blue) and after (red) UV exposure and the experimental values measured at a certain distance from the center of the droplet: (a) 780 µm, (b) 1440 µm, (c) 2130 µm, and (d) 2830 µm. (e) Comparision between the estimated heights and the measured heights of the fabricated waveguides, with the errors of less than 5%.

A 25 µL SU-8 droplet resulted in a base diameter of 7 mm and a contact angle of 39.4°. Their average measured heights were plotted on the estimated droplet profile after exposure. As the graph showed in Fig. 7 (e), the waveguide lengths were close to the estimated value with a standard deviation of less than 5%. This result demonstrated the repeatability and reliability of the proposed fabrication method.

C. Control of tip and base diameters

To investigate the tip size control of the DBE, tip and bottom diameters of the samples used in the previous session were measured and plotted in Fig. 8. Our preliminary results showed that the base diameter of the microneedle was determined by the diameter of the make aperture and did not change with different droplet volume, while the tip size showed a strong correlation with the droplet volume change.

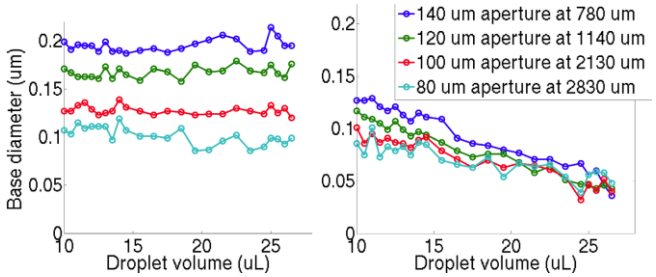

Figure 8. Base (left) and tip (right) size control via SU-8 droplet volume. Four aperture sizes, 140, 120, 100, and 80 µm in diameter at 780, 1140, 2130, and 2830 µm apart from the center of the droplet with 24 different volumes (10 to 27 µL) respectively.

V. CONCLUSION

A new fabrication method for making slanted microneedle structure called DBE method was proposed, and the preliminary experimental results were consisted with our analytical estimation. The control of the three parameters of the microneedle (length, tip and base diameters) was done by manipulating the droplet volume and the mask aperture design (the distance from the center and the diameter). The repeatability and controllability of the DBE method for microneedle fabrication were also demonstrated.

In future work, further improvement in a modeling of the SU-8 droplet with a consideration of solvent evaporation and SU-8 shrinkage after post baking must be done. Analytical model of the tip size with a droplet volume and a mask design (aperture size and a distance from the center of the droplet) is needed to understand the strength and limitation of the DBE method.

REFERENCES

[1] D. V. McAllister, P. M. Wang, S. P. Davis, J. H. Park, P. J. Canatella, M. G. Allen, and M. R. Prausnitz, "Microfabricated needles for transdermal delivery of macromolecules and nanoparticles: fabrication methods and transport studies," *Proceedings of the National Academy of Sciences of the United States of America*, vol. 100, no. 24, pp. 13755–13760, 2003.

[2] Y. Chen, W. Yang, Y. Huang, C. Fu, Y. Fu, and S. Tang, "Engineering a biomimetic villus array for in vitro 3-dimensional culture of intestinal epithelial cells," *Nano/Micro Engineered and Molecular Systems, 7th IEEE International Conference on*, pp. 230–233, 2012.

[3] T. Abaya, M. Diwekar, S. Blair, P. Tathireddy, L. Rieth, G. A. Clark, and F. Solzbacher, "Characterization of a 3D optrode array for infrared neural stimulation," *Biomedical Optics Express*, vol. 3, no. 9, pp. 2200–2219, 2012.

[4] E. S. Boyden, F. Zhang, E. Bamberg, G. Nagel, and K. Deisseroth, "Millisecond-timescale, genetically targeted optical control of neural activity," *Nature Neuroscience*, vol. 8, no. 9, pp. 1263–1268, Aug. 2005.

[5] K. Y. kwon and W. Li, "Integrated multi-LED array with three-dimensional polyer waveguide for optogenetics," *Micro Electro Mechanical Systems, IEEE 26nd International Conference on*, pp. 1–4, Jan. 2013.

[6] H. Huang and E. al, "Different fabrication methods of out-of-plane polymer hollow needle arrays and their variations," *J. Micromech. Microeng.*, vol. 17, no. 2, pp. 393–402, Jan. 2007.

[7] K. Kwon and W. Li, "Integrated slanted microneedle-LED array for optogenetics," *Medicine and Biology Society, IEEE 35th Annual International Conference on,* Jun. 2013, Submitted for publication.

[8] T. A. Duncombe, J. F. Parsons, and O. Bohringer, "Droplet transport on flat chemically heterogeneous surfaces via periodic wetting barriers and vibration," *Micro Electro Mechanical Systems, IEEE 23rd International Conference on*. 2010.

[9] Harris, J. W. and Stocker, H. "Spherical Zone (Spherical Layer)." *Handbook of Mathematics and Computational Science*. New York: Springer-Verlag, pp. 107-108, 1998.

[10] V. Fakhfouri, N. Cantale, G. Mermoud, J. Y. Kim, D. Boiko, E. Charbon, A. Martinoli, and J. Brugger, "Inkjet printing of SU-8 for polymer-based MEMS a case study for microlenses," presented at the *Micro Electro Mechanical Systems, IEEE 21st International Conference on*, 2008.

[11] SU-8 3000 Data Sheet - MicroChem, http://microchem.com/pdf/SU-8%203000%20Data%20Sheet.pdf.

[12] L. J. Guerin, M. Bossel, M. Demierre, S. Calmes, and P. Renaud, "Simple and low cost fabrication of embedded micro-channels by using a new thick-film photoplastic," *in Solid State Sensors and Actuators, IEEE International Conference on*, pp. 1419-1422, 1997.